*SLEEP*, 2025, **48**, 1–12
**doi:10.1093/sleep/zsaf151**
Advance Access publication 7 June 2025
**Original Article**

## Original Article

# The influence of peripheral glucose on sleep brain oscillations

Yu Lun[1], Manfred Hallschmid[1,2,3,4], Jan Born[1,2,3,4,5] and Niels Niethard[1,3,6,*]

[1]Institute of Medical Psychology and Behavioral Neurobiology, University of Tübingen, Tübingen, Germany
[2]German Center for Diabetes Research (DZD), Tübingen, Germany
[3]Institute for Diabetes Research and Metabolic Diseases of the Helmholtz Center Munich at the University Tübingen (IDM), Tübingen, Germany
[4]German Center for Mental Health (DZPG), Tübingen, Germany
[5]Center for Integrative Neuroscience, University of Tübingen, Tübingen, Germany
[6]Department of Cognitive Sciences, University of California, Irvine, Irvine, CA, USA

[*]**Corresponding author.** Niels Niethard, Institute of Medical Psychology and Behavioral Neurobiology, University of Tübingen, Tübingen, Germany. E-mail: niels.niethard@uni-tuebingen.de

## Abstract

**Study Objectives:** Previous research indicates a coupling of sleep-associated brain activity to peripheral glucose levels, such that ripple activity, a sign of increased hippocampal memory processing, is followed within 10 min by a dip in peripheral glucose levels. Whether there is respective negative feedback to the brain of peripheral glucose levels, or associated metabolic signaling, during sleep is not clear.

**Methods:** We tested the effects of systemic glucose administration as well as the effects of fasting (for 6 h vs. ad libitum feeding) on sleep and oscillatory signatures of memory processing during sleep, i.e. hippocampal ripples, cortical spindles and slow oscillations (SOs), using electroencephalography (EEG) from skull and local field potential recordings (LFP) from CA1 in male rats. Continuous monitoring of interstitial glucose concentrations in a subset of animals allowed the assessment of the temporal relationship between glucose fluctuations and oscillatory events.

**Results:** Hippocampal ripples and sleep spindles were accompanied by a transient decrease in peripheral glucose concentration. Neither glucose injection nor prior fasting influenced the macro-architecture of sleep during the subsequent 6 hours. Glucose injection (vs. water) increased spindle density. Prior fasting, compared with ad libitum feeding, increased numbers of ripples, spindles, SOs and of co-occurring SO-spindle events. Fasting also influenced SO-spindle phase-amplitude coupling, such that spindles occurred later during the SO upstate in fasted animals compared to those with ad libitum food access.

**Conclusions:** Our findings indicate a relatively tight-paced glucose-to-brain feedback loop during sleep that may affect memory processing in thalamocortical and hippocampal networks.

**Key words:** sleep; glucose; slow oscillation; sleep spindle; ripple



**Submitted for publication:** August 23, 2024; **Revised:** May 12, 2025

## Graphical Abstract

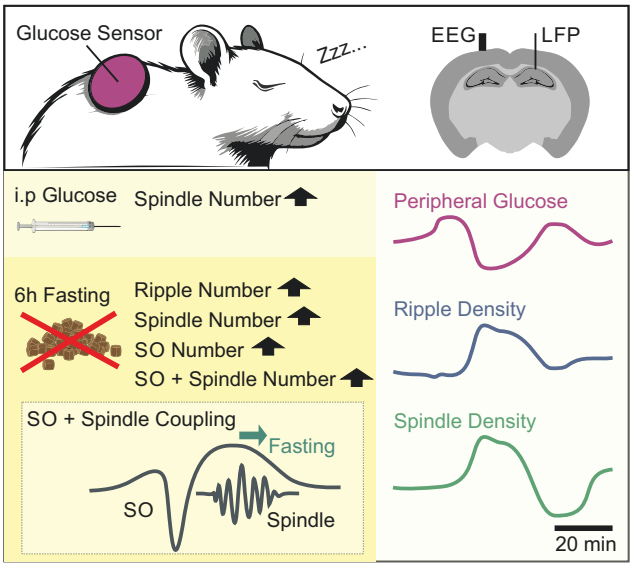


### Statement of Significance

Memory processing during sleep involves ripples, spindles, and slow oscillations that originate from hippocampal and thalamocortical networks during slow wave sleep. We recorded these oscillatory events together with peripheral glucose levels in freely behaving rats to explore how memory processing is coupled to metabolism. We found that hippocampal ripples and spindles are accompanied by a dip in glucose levels. Fasting, independently of glucose levels, increased ripples as well as slow oscillations and spindles and their co-occurrence. The findings point to a fine-tuned coupling between memory processing and body metabolism during sleep.

Memory formation is considered to be highly dependent on glucose homeostasis inasmuch glucose is the main energy source for neuronal computations and information processing in the brain [1–4]. Sleep supports memory consolidation [5, 6]. This function of sleep involves memory replay [7], a process that originates from hippocampal networks during Non-rapid eye movement (Non-REM) sleep. It is accompanied by hippocampal ripples [8], thalamocortical spindles [9], and neocortical slow oscillations (SOs) [10, 11].

Given the continuously changing energy demands of the memory processing brain during sleep, it seems reasonable to assume that peripheral glucose homeostasis is tightly coupled to neurophysiologic signatures of sleep-associated memory formation [12]. Indeed, two recent studies suggest that sleep-dependent neuronal activity that enables memory processing also exerts efferent control on peripheral glucose levels. Tingley et al. [13] observed in naturally sleeping rats that clusters of sharp wave-ripples recorded from the hippocampus reliably predicted a decrease in peripheral glucose concentrations within about 10 min. The transient down-regulation of peripheral glucose levels was not a mere reflection of generally increased neuronal firing activating local glucose transport to the brain but an active regulatory process which could be suppressed by inhibiting the lateral septum as the major conduit between the hippocampus and the hypothalamus. The second study showed in a large sample of healthy humans that stronger coupling of spindles to the SO upstate during nocturnal sleep predicts lower next-day fasting blood glucose levels [14]. Analyses of heart rate variability suggested a mediation of this relationship by shifting autonomic activity towards increased parasympathetic activity, ultimately enhancing insulin sensitivity.

While these studies provide strong evidence for the assumption of an intricate control of the body's glucose fluxes by the sleeping brain, it is presently unclear to what extent changes in peripheral glucose concentrations, in the sense of a negative feedback signal, acutely modulate key neuronal oscillations that orchestrate the brain's efferent glucoregulatory output. There is evidence that feeding behavior and blood glucose levels can affect the macro-architecture of sleep. Increased blood glucose levels have been found to decrease REM sleep [15] and high-carbohydrate diets reduced Non-REM sleep [16]. Moreover, hunger and blood glucose levels have been shown to regulate the excitability of brain areas relevant for memory consolidation [17–19]. The application of insulin on cultured hippocampal neurons suppressed intracellular $Ca^{2+}$ oscillations, which is in line with a role as a negative feedback signal [20, 21]. The hippocampus is an area particularly rich in glucose transporters and insulin receptors [22, 23]. Notably, we have previously shown in healthy humans that brain administration of insulin via the intranasal pathway before sleep increases nocturnal growth hormone concentrations and EEG delta power during Non-REM sleep [24].

Against this background, here we hypothesize a negative feedback mechanism wherein changes in peripheral glucose levels, or related metabolic alterations, provide feedback signals to the brain to specifically regulate neuronal activity linked to memory processing during sleep. Recording simultaneously cortical electroencephalography (EEG), hippocampal local field potentials (LFP) and interstitial glucose levels in freely behaving rats, we first

extended previous findings by Tingley et al. [13] in showing that not only hippocampal ripples but also spindles are accompanied by a dip in peripheral glucose concentrations, as has been found in a recent study in humans [25]. Relying on the direct manipulation of peripheral glucose concentrations by intraperitoneal (i.p.) injection (compared to water) in fasted (for 6 hours) or ad libitum fed rats, we moreover investigated whether transient increases in circulating glucose in the normal physiological range affect sleep and oscillatory signatures of memory processing during sleep. We found that glucose administration increased the number of spindles, but did not affect density of hippocampal ripples. Fasting distinctly increased ripple, spindle and SO density, as well as the numbers of SOs nesting spindles in their upstate and also delayed phase-amplitude coupling between SOs and spindles compared to ad libitum feeding. Our data provides first evidence that metabolic changes modulate ongoing memory processing during sleep.

# Methods

## Animals

Seven adult male Long Evans rats (Janvier, 310–320 g, 12 weeks of age) were used for the analysis. Rats were housed in groups of two per cage, except during the post-surgery recovery period, when they were kept individually. They were housed in cages with controlled temperature (22 ± 2°C) and humidity (45%–65%) on a 12-h light/12-h dark cycle (lights on at 06:00 am), with free access to water and food until the recording session. During the session, they were either fasted or had ad libitum access to food, depending on the specific conditions. All experimental procedures were approved by the local institutions in charge of animal welfare (Regierungspraesidium Tübingen, State of Baden-Wuerttemberg, Germany).

## Design and general procedures

Fig. 1 provides an overview of design and procedures. Rats ($n = 7$) were either fasted or given ad libitum access to food from 00:00 am onward. At 07:00 am, i.e., at the beginning of the rest period, the animals received an i.p. injection of either a 20% glucose solution (glucose dissolved in water at 1.5 g/kg body weight; B. Braun, Germany) or an equivalent dose of sterile water (control condition; Ampuwa, Fresenius Kabi, Germany). Water was used instead of saline to avoid potential interference with metabolic processing. EEG and LFP signals were recorded for the following six hours (07:00 am to 01:00 pm). In a subset of rats ($n = 4$), interstitial glucose concentration was monitored continuously by a glucose sensor (FreeStyle Libre 3, Abbott, USA) and EEG signals were recorded from 00:00 am to 06:00 am and 07:00 am to 01:00 pm. All animals were food-deprived during the morning (07:00 am to 01:00 pm) recording sessions. Each condition (Ad libitum-Glucose, Ad libitum-Control, Fasted-Glucose, Fasted-Control) was repeated two to three times, with the order counterbalanced across animals. Between recording sessions, animals were left in their home cage for one day of recovery.

## Surgical procedures and histology

Prior to surgery, rats were given an i.p. injection of anesthetic mixture (0.005 mg/kg fentanyl, 2 mg/kg midazolam and 0.15 mg/kg medetomidine) following quick isoflurane induction (3%–4% in 0.1 L/min $O_2$). Rats were positioned in the stereotaxic frame, and the skull was exposed. The entire surgery was carried out under isoflurane maintenance (0.5%–1%). For EEG recordings, four stainless steel screw electrodes (PlasticOne, USA) were implanted: two frontal electrodes (AP: + 2.6 mm, ML: ± 1.5 mm, relative to bregma), one parietal electrode (AP: – 2.0 mm, ML: – 2.5 mm, relative to bregma) and one occipital electrode (AP: –10.0 mm, ML: 0 mm, relative to bregma), serving as reference electrode. Additionally, two wires were implanted bilaterally to record LFP signals in the dorsal hippocampus (AP: – 4.3 mm, ML: ± 2.8 mm, DV: – 2.3 mm, relative to bregma).

For electromyographic (EMG) recordings, two wires were implanted in the neck muscle. Electrodes were inserted into a six-pin electrode pedestal (PlasticOne, USA) and anchored with cold polymerizing dental resin. During surgery, the animals were injected with 1 ml saline solution to prevent dehydration, and carprofen (5 mg/kg) was injected subcutaneously for three consecutive days. Rats were single-housed in their home cages and recordings were conducted after at least seven days of recovery.

Correct placement of LFP electrodes was verified by histology after completion of the experiments (Figure S1). Here, the rats were perfused intracardially with PBS followed by 4% paraformaldehyde (PFA). After decapitation, the brains were removed and immersed in the 4% PFA for two to three days. Coronal sections of

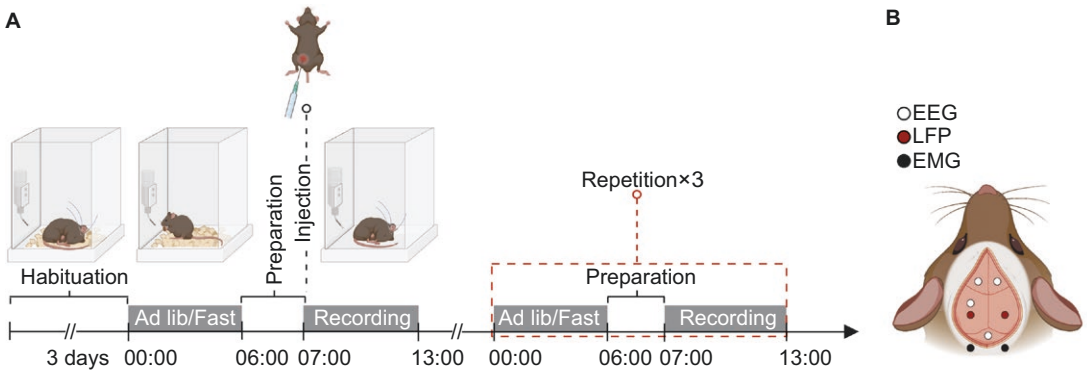


**Figure 1.** Experimental procedures. (A) Following 3 d of habituation, rats ($n = 7$) were placed in recording boxes for 6 h during the second half of the dark period (starting at 00:00 am); they had either ad libitum food access (Ad lib) or were fasted (Fast). In a subset of rats ($n = 4$), continuous interstitial glucose concentration was monitored using an attached glucose sensor. At 07:00 am, 1 h after lights on, the animals received an i.p. injection of either glucose or sterile water, and EEG and LFP signals were recorded for the next 6 h (07:00 am to 01:00 pm). All animals were food-deprived during this recording session. Between recording sessions, animals were left in their home cage for 1 d. Each condition (Ad libitum-Glucose, Ad libitum-Control, Fasted-Glucose, Fasted-Control) was repeated 2–3 times, with the order counterbalanced across animals. (B) Illustration of EEG (white dots), LFP (red dots) and EMG (black dots) electrode locations. The figures A and B were created with BioRender.com.

70–80 µm were made on a vibratome. The slices were stained with toluidine blue and examined under a light microscope.

## Electrophysiological recordings and procedures

Before recording sessions, rats were habituated to the recording box (stainless steel, 30 × 30 cm, height: 40 cm) for three days (from 07:00 am to 01:00 pm) with electrodes connection through a swiveling connector to an amplifier (Model 15A54, Grass Technologies, USA). On the next day, EEG, EMG, and LFP signals were recorded. All signals were continuously recorded and digitally processed using a CED Power 1401 converter and Spike2 software (Cambridge Electronic Design, UK). EEG signals were filtered between 0.1 and 300 Hz. LFP signals were filtered between 0.1 and 1,000 Hz. EMG signals were filtered between 30 and 300 Hz. All signals were sampled at 1 kHz.

## Animal preparation and intraperitoneal injection

Rats were handled for seven consecutive days for 10 min. During handling, rats were also habituated to the injection position by wrapping their body gently with a towel and holding them with their nose towards the ground. After three habituation days, prior to connecting them to the recording system, rats were wrapped and positioned to undergo simulated injection, that is, touching the injection site with a wooden tip of a cotton swab. This procedure minimized stress in the real injection sessions.

## Continuous glucose monitoring

A glucose-monitoring sensor (FreeStyle Libre 3, Abbott, USA) was used to measure peripheral glucose concentrations in four rats. For implantation, rats were anaesthetized lightly using isoflurane. The fur in the interscapular region was shaved, revealing the underlying skin. After disinfection, the sensor applicator was placed on the prepared area. The sensor was slowly pressed downward against the skin. The applicator was removed after inserting the sterile filament beneath the skin. Transparent dressing film (Tegaderm, 3M, United States) and medical adhesive bandage (Leukoplast hospital, BSN medical GmbH, Germany) was applied to keep the sensor in place. The sensor yielded glucose readings in mg/dL every five minutes. Glucose sensor readings were confirmed twice on separate days in one additional rat, which was injected glucose (1.5 g/kg body weight). After 10 min, when glucose concentration is expected to reach the maximum, blood was collected by pricking the tail vein with a lancet (Safty-Lancet,18G, Sarstedt, Germany). The blood drop was absorbed by the glucometer strip (Accu-Chek Performa, Germany) and the glucometer displayed the glucose reading in mg/dl. The calibration was repeated on a second day.

## Sleep stage classification

Sleep stages (including Non-REM and REM sleep) and wakefulness were determined offline through visual inspection using 10-s windows based on standard criteria. Wakefulness was defined by mixed-frequency EEG accompanied by relatively high EMG activity; Non-REM sleep by predominant high-amplitude delta activity (< 4.0 Hz), the presence of sleep spindles (11–16 Hz) and diminished EMG activity; REM sleep by predominant theta activity (5.0–10.0 Hz), phasic muscle twitches, and minimal EMG activity.

## Offline detection of SOs, spindles, and ripples

To detect SOs, EEG signals were first filtered between 0.5 and 4 Hz using a zero-phase shift (3rd order Butterworth filter). All zero crossings of the filtered signal during Non-REM sleep were then identified. The duration between two consecutive positive-to-negative zero crossings had to be between 0.5 and 2 s. For each remaining event, the peak-to-peak amplitude between the most negative and the most positive peak of the respective events had to be at least 66% of the amplitude of all previously detected events to be considered an SO.

For spindle detection, the signals were filtered between 11 and 16 Hz with a zero-phase shift (3rd order Butterworth filter). The amplitude was extracted based on the absolute value of the Hilbert-transformed filtered signal. Spindles were identified as events exceeding at least 1.6 SD of the mean amplitude of the filtered signal during Non-REM sleep for at least 0.5 s. Additionally, the amplitude had to surpass 2 SDs for at least 0.25 seconds and reach 2.2 SDs at least once.

Spindles co-occurring with SOs were defined as spindles occurring within a time window of ± 2.5 s around the most negative peak of an SO. To extract the phase-amplitude coupling between SOs and spindles, the SO signals were first filtered between 1.8 and 2 Hz. The phase of the filtered signal was then extracted using the built-in "angle" and "hilbert" functions of Matlab (Mathworks, USA). The respective maximum spindle amplitudes were used as reference points to extract the corresponding phase.

Ripples were detected only in LFP signals, using a zero-phase shift bandpass filter between 80 Hz and 300 Hz. The absolute value of the Hilbert transform of the filtered signal was used to identify the amplitude of the respective frequency bands. Ripples were detected whenever the amplitude of the signals exceeded 2 SDs of the mean amplitude during Non-REM sleep and wakefulness for at least 30 ms but not longer than 500 ms. Additionally, the signal had to cross a threshold of 4 SDs at least once. To compensate for potential artifacts from muscle movements, the same procedure was applied to EMG signals. Events in the LFP signals were considered only if they did not co-occur with control events detected in any of the EMG signals. Data from one animal that was recorded for 24h continuously without any intervention is provided in Figure S2.

## Statistical analyses

Cross-correlations were calculated using the "crosscorr" function of the statistics toolbox in Matlab (Mathworks, USA) and relied on data from four animals that repeatedly underwent the different conditions (Ad libitum-Glucose, $n = 8$ sessions; Ad libitum-Control, $n = 6$ sessions; Fast-Glucose, $n = 7$ sessions; Fast-Control, $n = 7$ sessions). These cross-correlations were computed between time series of glucose measurements and the occurrence rate (density) of the respective sleep-related events, with data binned into 5-minute intervals to match the sampling rate of the glucose sensor. Following previously described procedures [13], the cross-correlations were calculated on the first derivative of the high-pass (0.000025 Hz) filtered glucose data. To control for the influence of brain state transitions, partial cross-correlations were performed using Matlab's built-in function "regress." The cross-correlations were accordingly calculated for glucose data after regressing out (by respective binary control vectors) (i) wakefulness, (2) Non-REM, and (3) REM sleep, during each 5-minute interval. To compare the resulting cross-correlation functions against zero, cluster-based permutation tests were performed using the "clust_perm1" function from the Mass_Univariate_ERP_Toolbox [26]. This approach was used to determine the significance of distinct peaks in the cross-correlation functions and to simultaneously reduce the risks of Type 1 error associated with multiple comparisons [27].

The interventional sessions were implemented in seven animals according to a two-by-two factorial design, resulting in four experimental conditions: Ad libitum-Glucose ($n = 19$ sessions), Ad

libitum-Control ($n$ = 20 sessions), Fasted-Glucose ($n$ = 20 sessions), Fasted-Control ($n$ = 20 sessions).

All group comparisons were run with a two-by-two linear mixed-effects model using the "fitlme" function in Matlab (Mathworks, USA). A linear mixed-effects model was first fitted with both Glucose/Control and Ad libitum/Fasted as fixed effects and their interaction included in the model. A random intercept for Animal was included to account for repeated measurements within animals. Next, a reduced model, excluding the interaction term, was fitted. The interaction between diet and glucose condition was tested by comparing the full model (with interaction) to the reduced model (without interaction) using the "compare" function of Matlab (Mathworks, U.S.A.). If the $p$-value for the interaction term was > .05, the interaction was considered non-significant, and the reduced model was retained for subsequent analyses. Main effects of Glucose/Control and Ad libitum/Fasted were tested by comparing the models with and without respective main effects. These analyses were performed on 20-minute time bins. Basically, the same linear mixed-effects model approach was applied to additional data from two hours of concatenated Non-REM sleep (with averaged data across the repeated measurements of one condition for each animal).

Statistical comparisons of SO-spindle phase-amplitude coupling between the four conditions were calculated using the Circular Statistics Toolbox for Matlab [28]. Comparisons relied on linear mixed models as described above for the density comparison of the respective event of interest with the main differences that circular data was subtracted by the maximum of the respective dataset to allow the usage of the linear mixed model approach. To analyze the occurrence of spindles and SOs, events were collapsed across all channels. A $p$-value < .05 was considered significant.

# Results

## Temporal correlation between sleep oscillations and peripheral glucose concentrations

In a subset of animals we aimed at replicating recent findings by Tingley et al. [13] which provided the basis for the present study in showing that clusters of hippocampal ripples are followed by a transient decrease in peripheral glucose levels. In these animals ($n$ = 4), sleep was assessed in a total of 56 sessions (including 28 pre-injection sessions in which rats were either fasted or had ad libitum access to food, and 28 post-injection sessions, i.e., after either glucose or water injection). We performed cross-correlation analyses between time series (5-min bins) of interstitial glucose concentration assessments and density measures of hippocampal ripples, spindles, and SOs. In order to remove contributions of brain state transitions which themselves exhibited a strong cross-correlation with interstitial glucose levels (Fig. 2A), we performed partial cross-correlations which included three control variables that binarily encoded periods of wakefulness, Non-REM sleep, and REM sleep for each 5-minute bin (Fig. 2B).

The mean cross-correlation function between hippocampal ripples and glucose levels showed a pronounced negative peak at a + 5-minute lag (max $r$ = –0.068 ± 0.026) which revealed to be significant in a cluster spanning –10 to + 10 minutes ($p$ < .001, Fig. 2C, top). Similarly, we observed a significant negative correlation between spindle density and glucose levels at lags between –10 and + 10 minutes peaking at –10 minutes (max $r$ = –0.089 ± 0.019, $p$ < .001), followed by a positive correlation between + 20 and + 30 minutes peaking at + 20 minutes (max $r$ = 0.087 ± 0.015, $p$ < .001) (Fig. 2C, middle). For SOs, a pronounced positive correlation occurred at + 25 minutes (max r = 0.0567 ± 0.016, $p$ < .001) (Fig. 2C, bottom). Due to the relatively small sample size, only cross-correlations between spindle density and glucose levels remained significant when cross-correlation functions were averaged for each animal (Fig. 2C).

## Glucose injections and fasting do not modulate sleep architecture

Effects of glucose vs. water injection and of fasting vs. ad libitum food access were analyzed in a total of 79 sessions in seven animals (Ad libitum-Glucose: 19; Ad libitum-Control: 20; Fasted-Glucose: 20; Fasted-Control: 20). Glucose monitoring in the respective subset of animals confirmed that i.p. glucose compared to water control injections transiently increased interstitial glucose levels, triggering a maximum around 10–15 min later while 6-hour fasting significantly reduces interstitial glucose levels ($\chi^2(1) = 8.90$, $p = .0028$ for the Ad libitum/Fasted main effect; Fig. 3A and B). Time in Non-REM and REM sleep was analyzed for 20-min-bins during the 6-hour post-injection interval. There was no consistent effect of glucose injection on Non-REM or REM sleep duration across the entire six-hour interval (for the Glucose/Control main effect, and interaction effects with Ad libitum/Fasted; all $p \geq .69$; Fig. 3C) nor during any of the 20-minute intervals (all $p \geq .11$ for the Glucose/Control main effect; Figure S3). Also, glucose injection did not affect onsets of the first Non-REM and REM sleep periods (Non-REM: $\chi^2(1) = 0.51$, $p = .47$; REM: $\chi^2(1) = 1.07$, $p = .30$ for the Glucose/Control main effect; Fig. 3D).

Ad libitum access to food vs. fasting in the 6 hours prior to recording likewise did not influence sleep macro-architecture. Both conditions were closely comparable with regard to duration of Non-REM and REM sleep (all $p > .22$ for Ad libitum/Fasted main effect, $p > .78$ for respective interactions with Glucose/Control; Fig. 3C) and onset latencies of Non-REM and REM sleep (Non-REM: $\chi^2(1) = 0.002$, $p = .96$; REM: $\chi^2(1) = 3.46$, $p = .06$ for the Ad libitum/Fasted main effect; Fig. 3D).

## Effects of glucose injections on ripples, spindles, and SOs

To assess the effects of changes in peripheral glucose concentrations on sleep oscillations during Non-REM sleep, we analyzed EEG and LFP recordings, focusing on the occurrence of hippocampal ripples in the LFP and of sleep spindles and SOs in the EEG. To account for variations in the total amount of Non-REM sleep during the six-hour interval, we limited our analysis to events that occurred within the first two hours of concatenated Non-REM sleep.

Glucose compared to water injection did not affect the number of ripples or SO events during the two-hour concatenated Non-REM sleep interval (Glucose/Control main effect, $\chi^2(1) = 1.91$, $p = .17$ and $\chi^2(1) = 0.007$, $p = .93$, for ripples and SOs respectively; Fig. 4A and C). However, glucose injection increased the number of spindles in the two hours of concatenated Non-REM sleep (mean ± SEM spindles, Glucose, 283.98 ± 17.71, Control 256.44 ± 18.48 Glucose/Control main effect, $\chi^2(1) = 4.54$, $p = .031$; Fig. 4B). Interestingly, the increase in spindle density after glucose injection was already observed between 40 to 65 minutes of Non-REM sleep and remained significant even after Bonferroni correction (Glucose/Control main effect 40–65 minutes: $p \leq .03$; Fig. 4B) and during this time window, the Glucose/Control × Ad libitum/Fasted interaction also reached significance ($p \leq .05$).

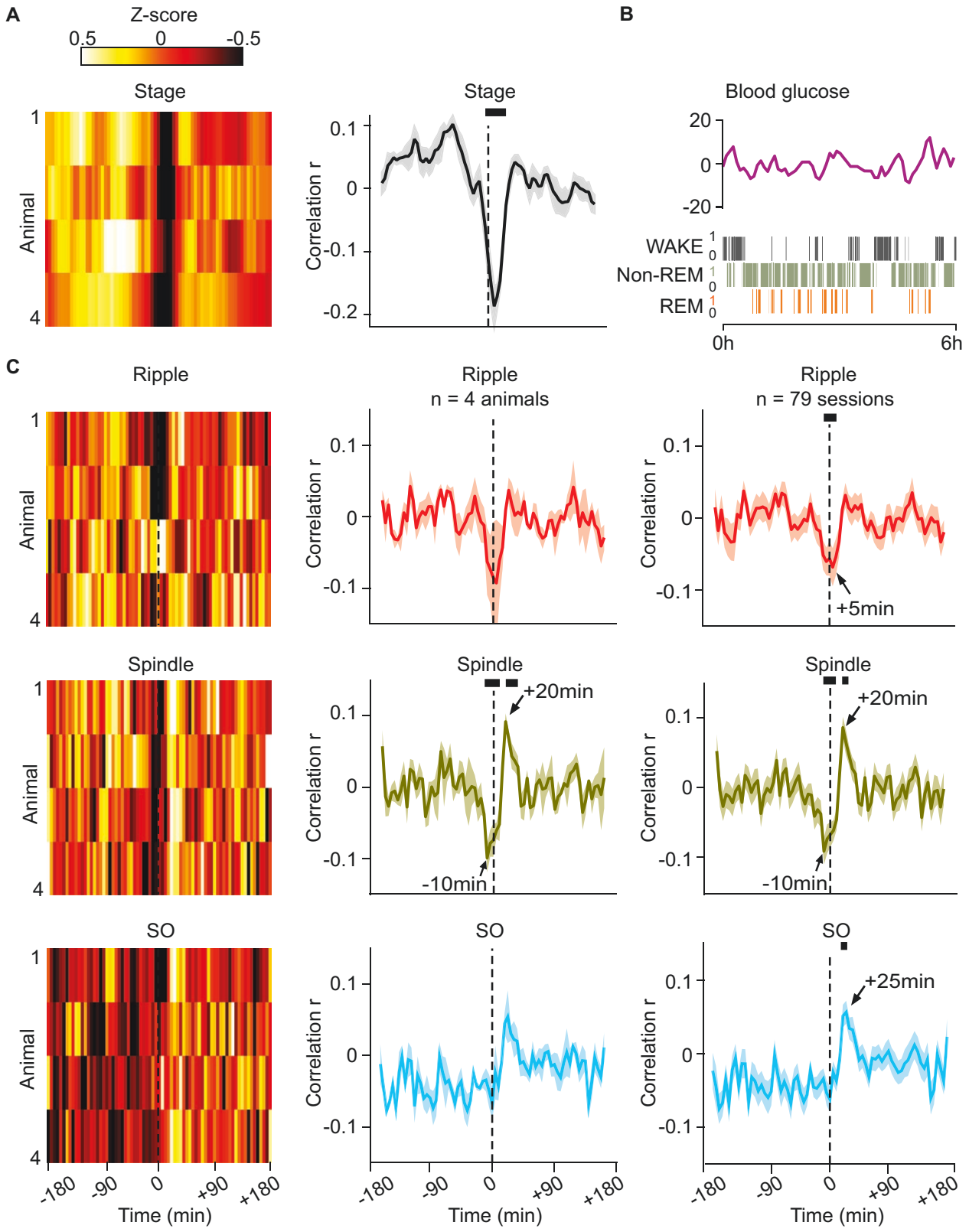


**Figure 2.** Partial cross-correlations between sleep oscillations and peripheral glucose concentrations. (A) Left: Z-transformed cross-correlation functions computed separately for each animal between glucose concentrations and a binary vector indicating periods of Non-REM sleep (coded as 1) and wakefulness and REM (both coded as 0, given the absences of the oscillations of interest in these states). Right: Corresponding average cross-correlation function across animals (mean ± SEM; $n = 4$ animals). (B) Example 6-hour glucose trace with corresponding binary vectors coding for wakefulness, Non-REM, and REM sleep, which were used as control variables in the partial cross-correlation analysis shown in (C). (C) Left: Animal-wise z-transformed partial cross-correlation functions. Middle: Partial cross-correlation functions averaged across animals (mean ± SEM, $n = 4$ animals), and (right) averaged across sessions ($n = 79$). Significance was assessed using a cluster-based permutation test and significant clusters ($p \leq .05$) are indicated by black horizontal bars.

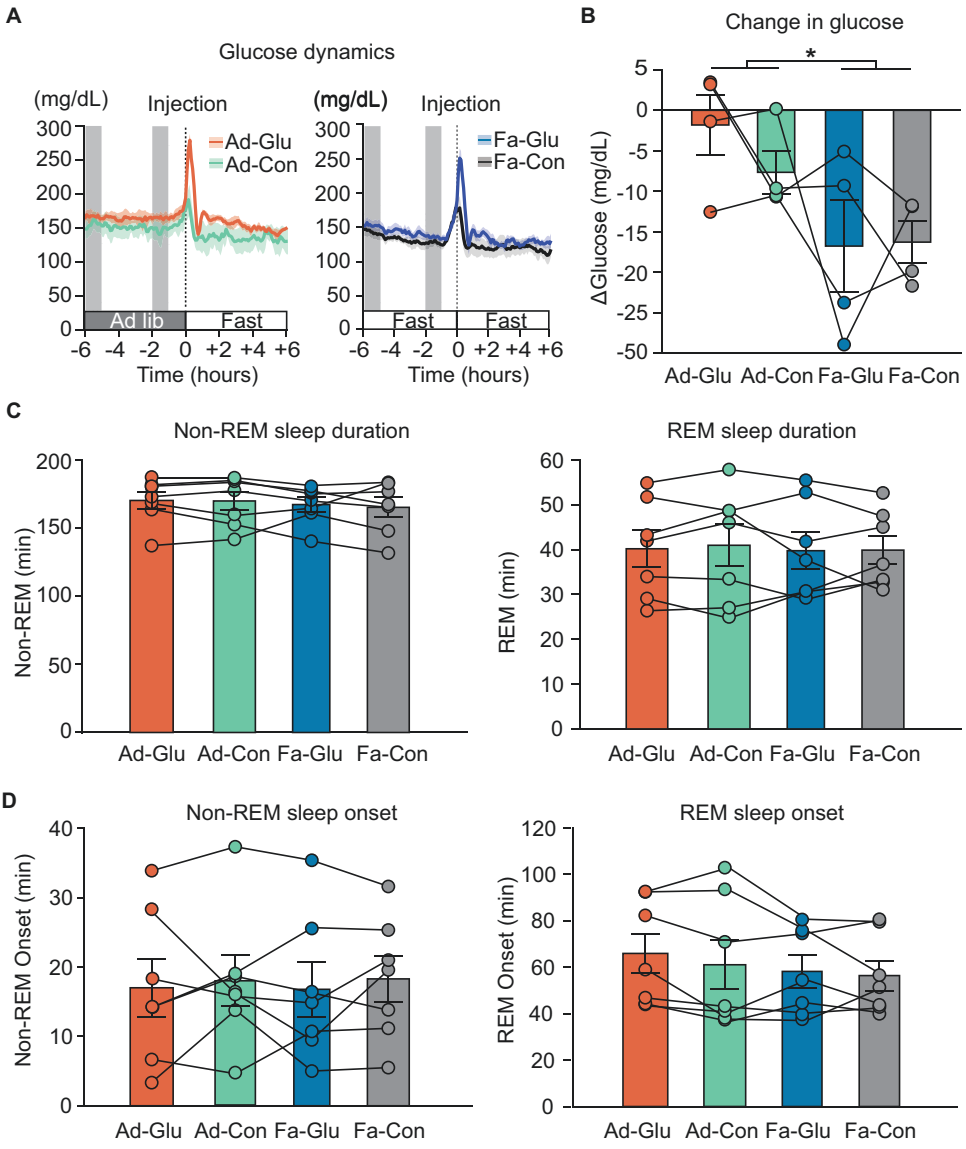


**Figure 3.** Effects of glucose vs. water injection and pre-injection fasting vs. ad libitum feeding on sleep architecture. (A) Interstitial glucose levels (mean ± SEM) before and after injections of glucose (Glu) or water (Con) confirmed an increase in glucose concentrations following glucose injection compared to water. Glucose was continuously monitored for six hours prior to injection (–6 to 0 hours), during which animals either had ad libitum access to food (Ad lib, left) or were fasted (Fast, right). After the injection (0 to +6 hours), monitoring continued for another six hours (Ad libitum-Glucose, $n = 8$ sessions; Ad libitum-Control, $n = 6$ sessions; Fast-Glucose, $n = 7$ sessions; Fast-Control, $n = 7$ sessions acquired in 4 animals). The dashed line at time 0 marks the injection point for both glucose and water. (B) Change in interstitial glucose levels (ΔGlucose) between the time intervals – 6 to – 5 hours and – 2 to – 1 hours relative to injection (gray areas in (A)), across the four experimental conditions: Ad libitum-Glucose (Ad-Glu), Ad libitum-Control (Ad-Con), Fasted-Glucose (Fa-Glu), and Fasted-Control (Fa-Con). Bars show group means ± SEM; individual animal values are shown as connected dots ($n = 4$ animals). (C) Total sleep duration in the 6-hour post-injection interval (0 to + 6 hours) for Non-REM (left) and REM sleep (right), across the four conditions. Bars represent group means ± SEM; individual data points with trajectories are overlaid ($n = 7$ animals). (D) Sleep onset latency (mean ± SEM for [$n = 7$ animals]) for Non-REM (left) and REM sleep (right), measured in minutes after injection. No significant differences in sleep onset or sleep duration were observed between conditions. * $p < .05$.

## Effects of fasting on ripples, spindles, and SOs

Pre-injection fasting compared to ad libitum food access was followed by an increase in ripple density during the first two hours of concatenated Non-REM sleep (mean ± SEM ripples, Ad libitum, 4768.02 ± 550.35, Fasted, 5624.25 ± 495.05; $\chi^2(1) = 5.39$, $p = .02$ for the Ad libitum/Fasted main effect; Fig. 4A). This effect was already visible after 45 min subsequent to the injection time point ($\chi^2(1) = 3.93$, $p = .047$), and independent of whether the animals received glucose or water (Glucose/Control × Ad libitum/Fasted: $\chi^2(1) = 0.05$, $p = .82$). It was essentially identical when periods of wakefulness were included in the 120-min interval ($\chi^2(1) = 9.10$, $p = .002$ for the Ad libitum/Fasted main effect).

Like ripple density, also spindle density was increased after fasting (compared to ad libitum food access) during the first two hours of concatenated Non-REM sleep (mean ± SEM spindles, Ad libitum, 257.77 ± 17.23, Fasted, 282.65 ± 20.28; $\chi^2(1) = 3.86$, $p = .049$ for the Ad libitum/Fasted main effect; Fig. 4B). Again the effect did not depend on whether the animals received glucose or water (Glucose/Control × Ad libitum/Fasted: $\chi^2(1) = 1.24$, $p = .27$). Interestingly, the increase in spindle density after glucose injection was already observed between 40 to 65 minutes of Non-REM

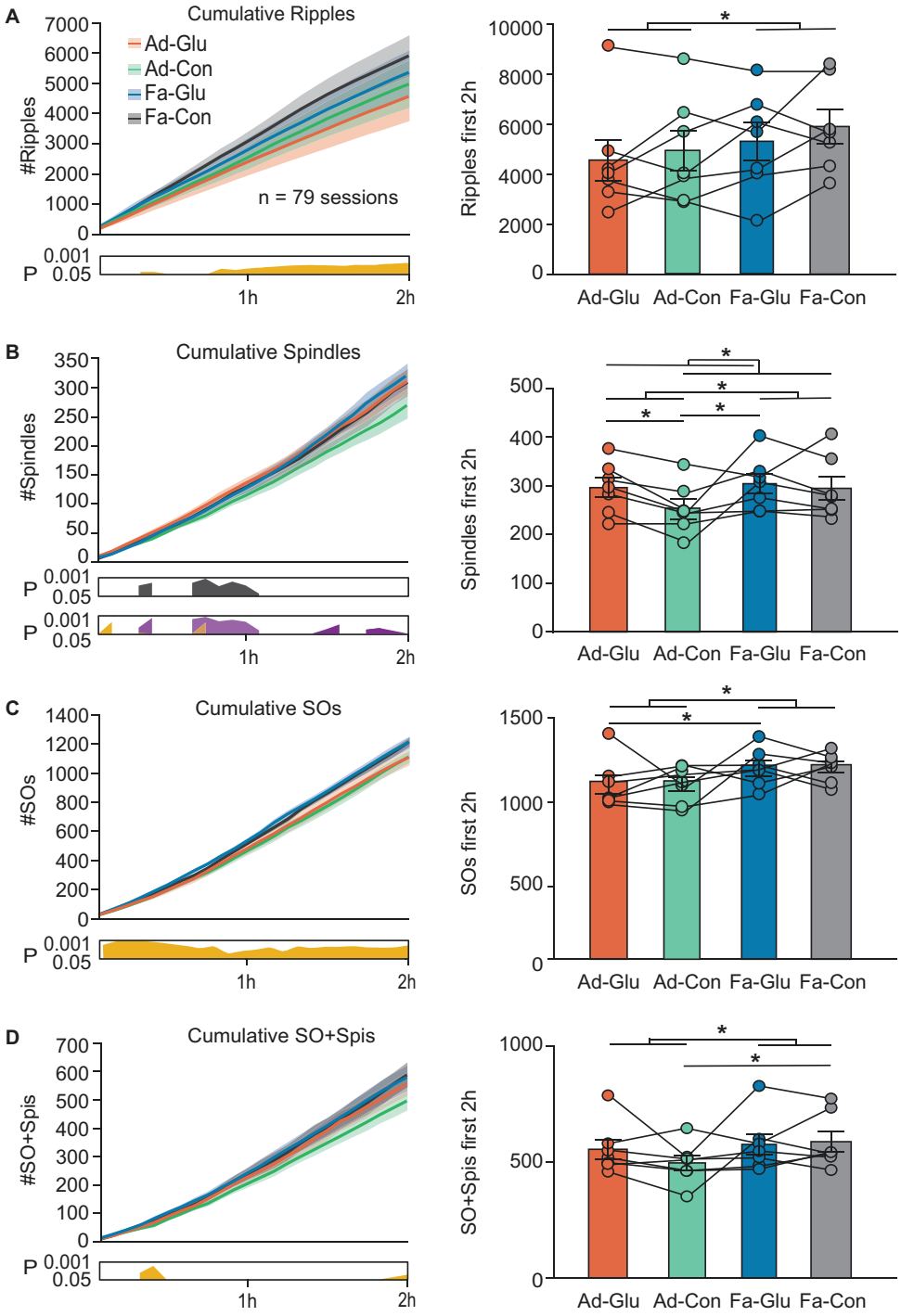


**Figure 4.** Effects of glucose and fasting on the density of ripples, spindles, SOs and on SO-spindle co-occurrence. (A) Left: Cumulative number of hippocampal ripples during the first 2 hours of concatenated Non-REM sleep across the four experimental conditions: Ad libitum-Glucose (Ad-Glu, $n = 19$ sessions), Ad libitum-Control (Ad-Con, $n = 20$ sessions), Fasted-Glucose (Fa-Glu, $n = 20$ sessions), and Fasted-Control (Fa-Con, $n = 20$ sessions). Colored bars below indicate significant effects from a two-by-two linear mixed-effects model: purple for the main effect Glucose/Control, yellow for the main effect Ad libitum/Fasted. Right: Corresponding mean ± SEM ripple counts after 2 hours of concatenated Non-REM sleep for each condition, with individual animals plotted as connected dots ($n = 7$ animals). (B) Same as in (A) but for spindles and gray bars below additionally indicate significant Glucose/Control × Ad libitum/Fasted interactions. (C and D) Same as in (A), but for SOs and co-occurring SO-spindle events. Shaded areas and error bars represent mean ± SEM. * $p < .05$

sleep and remained significant even after Bonferroni correction (Glucose/Control main effect 40–65 minutes: $p \leq .03$; Fig. 4B). During this time window, the Glucose/Control × Ad libitum/Fasted interaction also reached significance, but this effect did not survive Bonferroni correction.

Fasting also yielded increased cumulative SO numbers, independently of the Glucose/Control injection condition (mean ± SEM SOs first 2h; Ad libitum, 1,107.99 ± 33.14; Fast, 1,208.51 ± 25.55, $\chi^2(1) = 6.24$, $p = .013$ for the Ad libitum/Fast main effect; Glucose/Control × Ad libitum/Fast: $\chi^2(1) = 0.0001$, $p > .99$; Fig. 4C). This

increase after fasting was already evident in the first 5 min of Non-REM sleep and persisted throughout the entire recording session (Ad libitum/Fasted main effect after the first 5 minutes: $\chi^2(1) = 6.31$, $p = .012$).

### Effects on SO-spindle events

Considering that spindles tend to nest into the upstate of SOs [29], we investigated how peripheral glucose injections and fasting affect SO-spindle co-occurrence and coupling. Whereas glucose injection did not affect the number of co-occurring SO-spindle events (Glucose/Control main effect: $\chi^2(1) = 0.83$, $p = .36$), this number was significantly increased after fasting compared to ad libitum food access after 120 minutes of Non-REM sleep (mean ± SEM SO-spindle events, Ad libitum, 525.74 ± 26.87, Fasted, 581.97 ± 30.54, $\chi^2(1) = 4.42$, $p = .035$ for the Ad libitum/Fasted main effect; Fig. 4D). The effect was already present during the interval 20 to 30 minutes ($p \leq .049$), but did not last throughout the entire two-hour interval of concatenated Non-REM sleep. It was independent of whether the animals received glucose or control injections (Glucose/Control × Ad libitum/Fasted: $\chi^2(1) = 2.02$, $p \geq .10$).

To more precisely characterize the coupling between SOs and spindles, we examined the phase-amplitude coupling between these two oscillations. Amplitude in the 11–16 Hz spindle frequency band was significantly modulated by the SO phase, consistently peaking in the up-phase of SOs in all four experimental conditions (Hodges-Ajne test, all $p < .001$). To analyze the coupling of the spindle amplitude maximum during the phase of the SO cycle we used linear mixed-effects model analyses (see Methods). The analyses revealed a significant main effect for the Ad libitum/Fasted factor reflecting that in the fasting condition the maximum spindle amplitude occurred significantly later during SO-phase and, thus, more closely to the SO-uphase peak in the Fasted (−13.30° ± 6.29°) compared with the Ad libitum condition (−35.70° ± 8.50°, $\chi^2(1) = 6.22$, $p = .012$) where the spindle maximum occurred earlier in the rising flank of the SO (Fig. 5). The main effect of Glucose/Control ($\chi^2(1) = 4.33$, $p = .51$) as well as the Ad libitum/Fasted × Glucose/Control interaction effect ($\chi^2(1) = 0.21$, $p = .65$) remained without significance in these analyses.

Control analyses assured that maximal amplitudes of spindles, SOs and ripples as well as overall power distributions during Non-REM sleep were comparable between conditions (all $p > .7$), excluding general EEG and LFP amplitude alterations as the drivers of the observed differences in spindle and SO density as well as SO-spindle co-occurrence.

## Discussion

Using electrophysiological recordings combined with interstitial glucose monitoring in rats, our study provides evidence that neurooscillatory hallmarks of the brain's memory processing during sleep are coupled to the metabolic regulation of peripheral body glucose levels. We first replicated the finding by Tingley et al. [13] that hippocampal ripple activity is negatively correlated with glucose levels. Extending these findings, we observed that sleep spindles are likewise accompanied by a transient decrease in glucose concentrations. In contrast, cross-correlation functions of SOs were mainly characterized by a pronounced positive peak at + 25 min. With regard to spindles and SOs, this pattern is consistent with recent findings in humans [25]. Testing possible afferent feedback effects through injection of glucose in the main set of our experiments, against our original hypothesis we did not find any evidence that ripples are downregulated by transient increases in peripheral glucose. However, we observed an afferent effect of glucose injection increasing spindle density. Fasting, on the other hand, enhanced the density of ripples, spindles and SOs as well as the co-occurrence of SOs and spindles. Additionally, fasting delayed the SO-spindle coupling by shifting spindle occurrence towards the peak of the SO upstate, a pattern previously shown to be negatively correlated with fasting blood glucose levels in humans the morning after sleep [14]. Our results are overall in line with the view that feedback signals originating from peripheral glucose concentrations contribute to the stability of Non-REM sleep physiology, including oscillatory signatures of memory processing in thalamocortical networks [30].

Our cross-correlation functions between interstitial glucose levels and hippocampal ripples and EEG spindles, respectively, with a negative peak correlation between −10 and + 5 min, indicate rather fast-acting pathways that mediate the central nervous suppression or peripheral glucose concentrations by ripples and spindles. Indeed, we cannot exclude an even faster glucose response, as glucose concentration was sampled online at a low rate, which limits temporal resolution. The time lag of 5 min we observed here for the glucose dip after hippocampal ripples is indeed shorter than that previously reported (of approximately 10 min) [13], with the difference between studies possibly related to differences in the sensitivity of the glucose sensors. The −10 min lag for the peak negative correlation between spindles and glucose concentration suggests that changes in glucose levels may even occur prior and potentially influence spindle activity. Consonant with Tingley et al. [13], the inspection of our data did not provide any hints that the cross-correlation functions substantially differed depending on whether the animals were fasted or ad libitum fed, further supporting the view of a fast efferent central nervous down-regulation of glucose in conjunction with the occurrence of ripples and spindles.

Rather than on efferent actions, our main focus was on afferent actions of transient changes of peripheral glucose concentrations on central nervous signatures of sleep and associated memory processing. In this context, our finding that glucose injection did not affect sleep macro-architecture seems at a first glance counterintuitive. Importantly, the dose of glucose applied here led to changes within the physiological range and was substantially lower than doses (2.5 g/kg) known to produce severe hyperglycemia in euglycemic rats [15]. Only such very high doses, when administered to young rats, shortened REM sleep [15]. In contrast, i.p. glucose administration within the physiological range appears to attenuate REM sleep only in old rats with poor glucose tolerance [31–33], but not in young rats with normal glucose homeostasis [31, 34]. Adding to this evidence, participants with impaired glucose homeostasis (e.g., diabetes and prediabetes) not only experience inadequate total sleep [35, 36, 37] and shorter REM sleep [35], but also lower spindle density compared with healthy subjects [38]. Here, testing healthy young adult rats, we found that glucose injection increased spindle density, suggesting that healthy brains tune their circuits to adapt to such exogenous glucose challenges within the physiological range. Whether such processes are altered in aged brains or due to diabetes needs to be investigated in appropriate animal models.

Importantly, we observed after fasting a distinct increase in the numbers of ripples, spindles, SOs, and of spindles nesting into the SO upstate, which all represent hallmarks of memory processing in thalamocortical networks during Non-REM sleep. Moreover, fasting shifted spindles to the peak of the SO upstate. Notably, these effects were seen independently of an additional

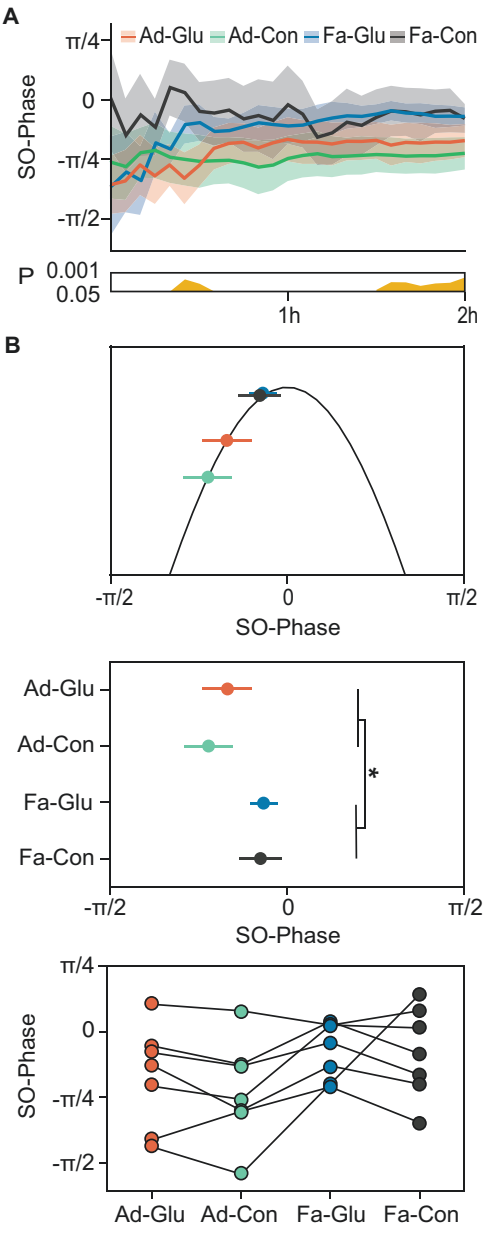


**Figure 5.** Effects of glucose and fasting on the phase-amplitude coupling between SOs and spindles. (A) Maximum spindle amplitude relative to the SO phase across concatenated 2-hour Non-REM sleep, displayed in 20-minute bins, for each of the four experimental conditions: Ad libitum-Glucose (Ad-Glu, $n = 19$ sessions), Ad libitum-Control (Ad-Con, $n = 20$ sessions), Fasted-Glucose (Fa-Glu, $n = 20$ sessions), and Fasted-Control (Fa-Con, $n = 20$ sessions). Bars below indicate significant effects from a two-by-two linear mixed-effects model for the main effect Ad libitum/Fasted (B) Top: Schematic illustration of the SO phase where spindle amplitude peaked. The SO upstate peak corresponds to 0 radians. Middle: Mean ± SEM of the SO phase at which maximum spindle amplitude occurred, shown for each condition ($n = 7$ animals). A significant main effect of the Ad libitum/Fasted condition is indicated. Bottom: Individual animal data showing repeated measures across conditions. * $p < .05$

glucose injection. This is a novel observation which altogether indicates that the metabolic state can massively bias the brain's machinery of memory processing during sleep, potentially offering one explanation for the beneficial effects of fasting on memory consolidation in humans [39]. It is also noteworthy that fasting affected the phase-amplitude coupling between spindles and SOs. This is all the more remarkable in light of recent findings in a large human cohort that identified the coupling between SOs and spindles as the most significant sleep predictor of next-day fasting glucose concentrations [14], and in principle concur with experimental results indicating the relevance of Non-REM sleep for glucose tolerance and insulin sensitivity [40]. In combination these findings suggest that synchronized processing in thalamocortical and hippocampal circuits—specifically cortical SO-spindle coupling and hippocampal ripples during Non-REM sleep—are key targets of metabolic feedback signals, influencing the neurocircuits involved in memory processing during sleep.

An open question remains whether the fasting-induced changes in phase–amplitude coupling, along with the observed increases in ripples, spindles, and SOs, translate into measurable alterations in cognitive functioning and memory consolidation during sleep. Previous work comparing SO-spindle phase-amplitude coupling in young and old adults suggests that a later occurrence of spindles relative to the SO-upstate—as observed here after fasting—is indeed associated with better memory performance [41]. On the other hand, increases in spindle densities—as observed here in glucose injected animals—are often associated with better memory performance [5, 6]. How the differential effects of glucose feedback and fasting combine to alter memory consolidation during sleep awaits experimental testing.

Another question to be addressed in further studies is the mediation of the observed metabolic feedback effects, and specifically those of glucose. One might speculate that they are a direct result of peripheral glucose crossing the blood-brain barrier via glucose transporters into the brain extracellular fluid (ECF) [42]. However, a single i.p. injection of a rather low dose of glucose, as in our study, is probably insufficient to induce prominent fluctuations in ECF glucose concentrations [43, 44]. ECF glucose concentrations are typically very stable, varying less than 2 mM between fasted and fed states [45, 46]. Rather than being transported into the CNS, blood glucose levels can also affect brain activity through glucose-sensing neurons. After i.p. injection, glucose is first absorbed by the peritoneum and transported via the portal vein, where glucose sensors can detect both hyper- and hypoglycemia through disparate neural pathways [47–51]. Finally, the effects of peripheral glucose on the brain may be mediated through several pathways, including the enhancement of insulin or other metabolic signals that are detected at the blood-brain barrier or within the brain itself [52, 53]. Additionally, vagal gut-to-brain signaling may play a role [54], potentially involving central vagal pathways that include the locus coeruleus—a key structure implicated in the generation of sleep spindles [55–57].

Despite the insights this study provides to interactions between peripheral glucose and oscillatory activity during sleep, three main limitations must be considered. First, the cross-correlation analysis is exploratory, as it is based on data from only four animals. Although we recorded 56 sessions, the between-animal variability and relatively short recording periods (6 hours) limit the conclusiveness of the observed effects. This is particularly relevant given the highly fragmented nature of rodent sleep, which complicates the dissociation between sleep stage and sleep-wake transitions and the specific oscillatory events of interest. The slow sampling rate of glucose signals (5-minute intervals) is a significant limitation too, as the underlying dynamics may operate on faster timescales. Moreover, blood glucose levels may offer a more precise measure of peripheral glucose dynamics related to brain activity. Finally, our approach does not allow us to disentangle the mediating mechanisms, which likely involve

insulin and other metabolic signals, as well as gut-to-brain signaling. These are promising avenues for future research.

Taken together, our findings support the view that, in addition to a gross coupling of sleep/wake states and associated food intake [58], brain activity and metabolism are coupled on a finer temporal scale, with signatures of hippocampal and thalamocortical memory processing occurring in close temporal proximity with decreases in peripheral glucose levels. However, these results do not exclude possibly more sustained as well as bidirectional interactions between sleep-related brain activity and glucose homeostasis. We here provide first time evidence that such transient changes in peripheral glucose may provide feedback to the brain within < 15 min, to mainly affect spindles, i.e., a signature of thalamocortical memory processing. How these indicators of fast brain-body regulation of glucose translate into conditions of impaired metabolic control like obesity and diabetes is an important question to be investigated in future studies.

## Supplementary material

Supplementary material is available at *SLEEP* online.

## Acknowledgments

We thank Ilona Sauter for valuable technical support.

## Funding

This work was supported by grants from the Deutsche Forschungsgemeinschaft to J.B. (FOR 5434), from the European Research Council to J.B. (ERC AdG 883098 SleepBalance), from the German Federal Ministry of Education and Research (BMBF) to the German Center for Diabetes Research (DZD e.V.), and from the Hertie Foundation, Network for Excellence in Clinical Neuroscience, to N.N. Y.L. gratefully acknowledges funding from the China Scholarship Council (CSC: # 201808080072). The funders had no role in study design, data collection and analysis, decision to publish, or preparation of the manuscript.

## Author contributions

Conception and design of the study: J.B and N.N.; Data Collection: Y.L. Data analysis: N.N.; Manuscript draft: Y.L. and N.N.; Manuscript editing: J.B., M.H. and N.N.

## Conflict of interest

*Financial disclosure:* The authors declare no conflict of interest. *Non-financial disclosure:* The authors declare no conflict of interest.

## Data availability statement

Requests for further information, data, and resources, should be directed to, and will be fulfilled by, the corresponding author.

## References

1. Hossain MS, Oomura Y, Fujino T, Akashi K. Glucose signaling in the brain and periphery to memory. *Neurosci Biobehav Rev.* 2020;**110**:100–113. doi:10.1016/j.neubiorev.2019.03.018
2. Harris JJ, Jolivet R, Attwell D. Synaptic energy use and supply. *Neuron.* 2012;**75**(5):762–777. doi:10.1016/j.neuron.2012.08.019
3. Jang S, Nelson JC, Bend EG, *et al*. Glycolytic enzymes localize to synapses under energy stress to support synaptic function. *Neuron.* 2016;**90**(2):278–291. doi:10.1016/j.neuron.2016.03.011
4. Rangaraju V, Calloway N, Ryan TA. Activity-driven local atp synthesis is required for synaptic function. *Cell.* 2014;**156**(4):825–835. doi:10.1016/j.cell.2013.12.042
5. Klinzing JG, Niethard N, Born J. Mechanisms of systems memory consolidation during sleep. *Nat Neurosci.* 2019;**22**(10):1598–1610. doi:10.1038/s41593-019-0467-3
6. Brodt S, Inostroza M, Niethard N, Born J. Sleep—a brain-state serving systems memory consolidation. *Neuron.* 2023;**111**(7):1050–1075. doi:10.1016/j.neuron.2023.03.005
7. Wilson MA, McNaughton BL. Reactivation of hippocampal ensemble memories during sleep. *Science.* 1994;**265**(5172):676–679. doi:10.1126/science.8036517
8. Diba K, Buzsáki G. Forward and reverse hippocampal place-cell sequences during ripples. *Nat Neurosci.* 2007;**10**(10):1241–1242. doi:10.1038/nn1961
9. Latchoumane CFV, Ngo HVV, Born J, Shin HS. Thalamic spindles promote memory formation during sleep through triple phase-locking of cortical, thalamic, and hippocampal rhythms. *Neuron.* 2017;**95**(2):424–435.e6. doi:10.1016/j.neuron.2017.06.025
10. Ramanathan DS, Gulati T, Ganguly K. Sleep-dependent reactivation of ensembles in motor cortex promotes skill consolidation. *PLoS Biol.* 2015;**13**(9):e1002263. doi:10.1371/journal.pbio.1002263
11. Marshall L, Helgadóttir H, Mölle M, Born J. Boosting slow oscillations during sleep potentiates memory. *Nature.* 2006;**444**(7119):610–613. doi:10.1038/nature05278
12. Peters A, Schweiger U, Pellerin L, *et al*. The selfish brain: competition for energy resources. *Neurosci Biobehav Rev.* 2004;**28**(2):143–180. doi:10.1016/j.neubiorev.2004.03.002
13. Tingley D, McClain K, Kaya E, Carpenter J, Buzsáki G. A metabolic function of the hippocampal sharp wave-ripple. *Nature.* 2021;**597**(7874):82–86. doi:10.1038/s41586-021-03811-w
14. Vallat R, Shah VD, Walker MP. Coordinated human sleeping brainwaves map peripheral body glucose homeostasis. *Cell Rep Med.* 2023;**4**(7):101100. doi:10.1016/j.xcrm.2023.101100
15. Sangiah S, Caldwell DF. Reduction of rapid eye movement (REM) sleep by glucose alone or glucose and insulin in rats. *Life Sci.* 1988;**42**(15):1425–1429. doi:10.1016/0024-3205(88)90052-5
16. St-Onge MP, Cherta-Murillo A, Darimont C, Mantantzis K, Martin FP, Owen L. The interrelationship between sleep, diet, and glucose metabolism. *Sleep Med Rev.* 2023;**69**:101788. doi:10.1016/j.smrv.2023.101788
17. Zanchi D, Depoorter A, Egloff L, *et al*. The impact of gut hormones on the neural circuit of appetite and satiety: a systematic review. *Neurosci Biobehav Rev.* 2017;**80**:457–475. doi:10.1016/j.neubiorev.2017.06.013
18. Al-Zubaidi A, Heldmann M, Mertins A, Jauch-Chara K, Münte TF. Influences of hunger, satiety and oral glucose on functional brain connectivity: a multimethod resting-state fMRI study. *Neuroscience.* 2018;**382**:80–92. doi:10.1016/j.neuroscience.2018.04.029
19. Tataranni PA, Gautier JF, Chen K, *et al*. Neuroanatomical correlates of hunger and satiation in humans using positron emission tomography. *Proc Natl Acad Sci USA.* 1999;**96**(8):4569–4574. doi:10.1073/pnas.96.8.4569
20. O'Malley D, Shanley LJ, Harvey J. Insulin inhibits rat hippocampal neurones via activation of ATP-sensitive K+ and large conductance Ca2+-activated K+ channels. *Neuropharmacology.* 2003;**44**(7):855–863. doi:10.1016/s0028-3908(03)00081-9
21. Jin Z, Jin Y, Kumar-Mendu S, Degerman E, Groop L, Birnir B. Insulin reduces neuronal excitability by turning on GABAA

channels that generate tonic current. *PLoS One*. 2011;**6**(1):e16188. doi:10.1371/journal.pone.0016188
22. Schulingkamp RJ, Pagano TC, Hung D, Raffa RB. Insulin receptors and insulin action in the brain: review and clinical implications. *Neurosci Biobehav Rev*. 2000;**24**(8):855–872. doi:10.1016/s0149-7634(00)00040-3
23. Lathe R. Hormones and the hippocampus. *J Endocrinol*. 2001;**169**(2):205–231. doi:10.1677/joe.0.1690205
24. Feld GB, Wilhem I, Benedict C, *et al*. Central nervous insulin signaling in sleep-associated memory formation and neuroendocrine regulation. *Neuropsychopharmacology*. 2016;**41**(6):1540–1550. doi:10.1038/npp.2015.312
25. Yang X, Fedumenti FT, Niethard N, Hallschmid M, Born J, Rauss K. Regulation of peripheral glucose levels during human sleep. *Sleep*. 2025;**48**(6):zsaf042. doi:10.1093/sleep/zsaf042
26. Bullmore ET, Suckling J, Overmeyer S, Rabe-Hesketh S, Taylor E, Brammer MJ. Global, voxel, and cluster tests, by theory and permutation, for a difference between two groups of structural MR images of the brain. *IEEE Trans Med Imaging*. 1999;**18**(1):32–42. doi:10.1109/42.750253
27. Maris E, Oostenveld R. Nonparametric statistical testing of EEG- and MEG-data. *J Neurosci Methods*. 2007;**164**(1):177–190. doi:10.1016/j.jneumeth.2007.03.024
28. Berens P. CircStat: a *MATLAB* toolbox for circular statistics. *J Stat Soft*. 2009;**31**(10):4–8. doi:10.18637/jss.v031.i10
29. Oyanedel CN, Durán E, Niethard N, Inostroza M, Born J. Temporal associations between sleep slow oscillations, spindles and ripples. *Eur J Neurosci*. 2020;**52**(12):4762–4778. doi:10.1111/ejn.14906
30. Niethard N, Hallschmid M. A sweet spot for the sleeping brain: Linking human sleep physiology and glucoregulation. *Cell Rep Med*. 2023;**4**(7):101123. doi:10.1016/j.xcrm.2023.101123
31. Stone WS, Wenk GL, Stone SM, Gold PE. Glucose attenuation of paradoxical sleep deficits in old rats. *Behav. Neural Biol*. 1992;**57**(1):79–86. doi:10.1016/0163-1047(92)90779-4
32. Oh YS, Seo EH, Lee YS, *et al*. Increase of calcium sensing receptor expression is related to compensatory insulin secretion during aging in mice. *PLoS One*. 2016;**11**(7):e0159689. doi:10.1371/journal.pone.0159689
33. Bracho-Romero E, Reaven GM. Effect of age and weight on plasma glucose and insulin responses in the rat. *J Am Geriatrics Soc*. 1977;**25**(7):299–302. doi:10.1111/j.1532-5415.1977.tb00641.x
34. Stone WS, Wenk GL, Olton DS, Gold PE. Poor blood glucose regulation predicts sleep and memory deficits in normal aged rats. *J Gerontol*. 1990;**45**(5):B169–B173. doi:10.1093/geronj/45.5.b169
35. Chen DM, Taporoski TP, Alexandria SJ, *et al*. Altered sleep architecture in diabetes and prediabetes: findings from the Baependi Heart Study. *Sleep*. 2024;**47**(1):zsad229. doi:10.1093/sleep/zsad229
36. Antza C, Kostopoulos G, Mostafa S, Nirantharakumar K, Tahrani A. The links between sleep duration, obesity and type 2 diabetes mellitus. *J Endocrinol*. 2022;**252**(2):125–141. doi:10.1530/joe-21-0155
37. Engeda J, Mezuk B, Ratliff S, Ning Y. Association between duration and quality of sleep and the risk of pre-diabetes: evidence from NHANES. *Diabet Med*. 2013;**30**(6):676–680. doi:10.1111/dme.12165
38. Yeung D, Talukder A, Shi M, *et al*. Differences in brain spindle density during sleep between patients with and without type 2 diabetes. *Comput Biol Med* . 2025;**184**:109484. doi:10.1016/j.compbiomed.2024.109484
39. Yang X, Miao X, Schweiggart F, *et al*. The effect of fasting on human memory consolidation. *Neurobiol Learn Mem*. 2025;**218**:108034. doi:10.1016/j.nlm.2025.108034
40. Tasali E, Leproult R, Ehrmann DA, Van Cauter E. Slow-wave sleep and the risk of type 2 diabetes in humans. *Proc Natl Acad Sci USA* 2008;**105**(3):1044–1049. doi:10.1073/pnas.0706446105.
41. Helfrich RF, Mander BA, Jagust WJ, Knight RT, Walker MP. Old brains come uncoupled in sleep: slow wave-spindle synchrony, brain atrophy, and forgetting. *Neuron*. 2018;**97**(1):221–230.e4. doi:10.1016/j.neuron.2017.11.020
42. Mueckler M. Facilitative glucose transporters. *Eur J Biochem*. 1994;**219**(3):713–725. doi:10.1111/j.1432-1033.1994.tb18550.x
43. McNay EC, Fries TM, Gold PE. Decreases in rat extracellular hippocampal glucose concentration associated with cognitive demand during a spatial task. *Proc Natl Acad Sci USA*. 2000;**97**(6):2881–2885. doi:10.1073/pnas.050583697
44. McNay EC, McCarty RC, Gold PE. Fluctuations in brain glucose concentration during behavioral testing: dissociations between brain areas and between brain and blood. *Neurobiol Learn Mem*. 2001;**75**(3):325–337. doi:10.1006/nlme.2000.3976
45. Harada M, Sawa T, Okuda C, Matsuda T, Tanaka Y. Effects of glucose load on brain extracellular lactate concentration in conscious rats using a microdialysis technique. *Horm Metab Res*. 1993;**25**(11):560–563. doi:10.1055/s-2007-1002177
46. Barnes MB, Lawson MA, Beverly JL. Rate of fall in blood glucose and recurrent hypoglycemia affect glucose dynamics and noradrenergic activation in the ventromedial hypothalamus. *Am J Physiol Regul Integr Comp Physiol*. 2011;**301**(6):R1815–R1820. doi:10.1152/ajpregu.00171.2011
47. Niijima A. Glucose-sensitive afferent nerve fibres in the hepatic branch of the vagus nerve in the guinea-pig. *J Physiol*. 1982;**332**(1):315–323. doi:10.1113/jphysiol.1982.sp014415
48. Hevener AL, Bergman RN, Donovan CM. Hypoglycemic detection does not occur in the hepatic artery or liver. *Diabetes*. 2001;**50**(2):399–403. doi:10.2337/diabetes.50.2.399
49. Bohland M, Matveyenko AV, Saberi M, Khan AM, Watts AG, Donovan CM. Activation of hindbrain neurons is mediated by portal-mesenteric vein glucosensors during slow-onset hypoglycemia. *Diabetes*. 2014;**63**(8):2866–2875. doi:10.2337/db13-1600
50. Fujita S, Donovan CM. Celiac-superior mesenteric ganglionectomy, but not vagotomy, suppresses the sympathoadrenal response to insulin-induced hypoglycemia. *Diabetes*. 2005;**54**(11):3258–3264. doi:10.2337/diabetes.54.11.3258
51. Saberi M, Bohland M, Donovan CM. The locus for hypoglycemic detection shifts with the rate of fall in glycemia. *Diabetes*. 2008;**57**(5):1380–1386. doi:10.2337/db07-1528
52. Gómez-Pinilla F. Brain foods: the effects of nutrients on brain function. *Nat Rev Neurosci*. 2008;**9**(7):568–578. doi:10.1038/nrn2421
53. García-Cáceres C, Quarta C, Varela L, *et al*. Astrocytic insulin signaling couples brain glucose uptake with nutrient availability. *Cell*. 2016;**166**(4):867–880. doi:10.1016/j.cell.2016.07.028
54. Han W, Tellez LA, Perkins MH, *et al*. A neural circuit for gut-induced reward. *Cell*. 2018;**175**(3):665–678.e23. doi:10.1016/j.cell.2018.08.049
55. Swift KM, Gross BA, Frazer MA, *et al*. Abnormal locus coeruleus sleep activity alters sleep signatures of memory consolidation and impairs place cell stability and spatial memory. *Curr Biol*. 2018;**28**(22):3599–3609.e4. doi:10.1016/j.cub.2018.09.054
56. Osorio-Forero A, Cardis R, Vantomme G, *et al*. Noradrenergic circuit control of non-REM sleep substates. *Curr Biol*. 2021;**31**(22):5009–5023.e7. doi:10.1016/j.cub.2021.09.041
57. Kjaerby C, Andersen M, Hauglund N, *et al*. Memory-enhancing properties of sleep depend on the oscillatory amplitude of norepinephrine. *Nat Neurosci*. 2022;**25**(8):1059–1070. doi:10.1038/s41593-022-01102-9
58. Schmid SM, Hallschmid M, Schultes B. The metabolic burden of sleep loss. *Lancet Diabetes Endocrinol*. 2015;**3**(1):52–62. doi:10.1016/S2213-8587(14)70012-9